Proceedings of the ASME 2014 International Mechanical Engineering Congress and Exposition
IMECE2014
November 14-20, 2014, Montreal, Quebec, Canada

IMECE2014-36909

VALIDATION OF COMPLEMENTARY FILTER BASED IMU DATA FUSION FOR TRACKING TORSO ANGLE AND RIFLE ORIENTATION

Ryan S. McGinnis
University of Michigan
Ann Arbor, MI, USA

Stephen M. Cain
University of Michigan
Ann Arbor, MI, USA

Steven P. Davidson
University of Michigan
Ann Arbor, MI, USA

Rachel V. Vitali
University of Michigan
Ann Arbor, MI, USA

Scott G. McLean
University of Michigan
Ann Arbor, MI, USA

N.C. Perkins
University of Michigan
Ann Arbor, MI, USA

ABSTRACT

Up-down and rifle aiming maneuvers are common tasks employed by soldiers and athletes. The movements underlying these tasks largely determine performance success, which motivates the need for a noninvasive and portable means for movement quantification. We answer this need by exploiting body-worn and rifle-mounted miniature inertial measurement units (IMUs) for measuring torso and rifle motions during up-down and aiming tasks. The IMUs incorporate MEMS accelerometers and angular rate gyros that measure translational acceleration and angular velocity, respectively. Both sensors enable independent estimates of the orientation of the IMU and thus, the orientation of a subject's torso and rifle. Herein, we establish the accuracy of a complementary filter which fuses these estimates for tracking torso and rifle orientation by comparing IMU-derived and motion capture-derived (MOCAP) torso pitch angles and rifle elevation and azimuthal angles during four up-down and rifle aiming trials for each of 16 subjects (64 trials total). The up-down trials consist of five maximal effort get-down-get-up cycles (from standing to lying prone back to standing), while the rifle aiming trials consist of rapidly aiming five times at two targets 15 feet from the subject and 180 degrees apart. Results reveal that this filtering technique yields warfighter torso pitch angles that remain within 0.55 degrees of MOCAP estimates and rifle elevation and azimuthal angles that remain within 0.44 and 1.26 degrees on average, respectively, for the 64 trials analyzed. We further examine potential remaining error sources and limitations of this filtering approach. These promising results point to the future use of this technology for quantifying motion in naturalistic environments. Their use may be extended to other applications (e.g., sports training and remote health monitoring) where noninvasive, inexpensive, and accurate methods for reliable orientation estimation are similarly desired.

INTRODUCTION

There is growing interest in monitoring the orientation of human body segments and sports equipment in applications including sports training and skill assessment [1–3], clinical assessment and rehabilitation [4,5], and remote health and performance monitoring [6]. For example, in [1], quantifying the orientation of a pitched baseball is paramount for resolving the release conditions used to assess the type and quality of a pitch. In [6], torso orientation during gait is shown to provide an indication of a subject's emotions which has exciting implications for remote health monitoring.

Traditionally, in sports, clinical, and research contexts, video-based techniques have been used to record and analyze a subject's motion and extract body segment orientation. In sports and clinical contexts, subject performance is often analyzed by reviewing video records [7]. Doing so allows coaches and clinicians to assess a subject's behavior with minimal set-up, and analysis of the performance is identical to visual assessment in real time. Unfortunately, traditional video records yield two-dimensional images with a fixed field of view, are not well suited for quantitative analyses (particularly for unconstrained tasks), and require an operator for recording. Moreover, subjects often know when they are being recorded which can influence their behavior. In research contexts, three-dimensional human motion is most often quantified using video-based motion capture (MOCAP), which relies on tracking

the three-dimensional position of subject-affixed reflective targets or infrared LEDs using an array of high speed, infrared cameras arranged around the perimeter of a capture volume, see for example [8]. This volume must be precisely calibrated prior to each testing session to yield accurate positional data which requires a skilled operator. Unfortunately, this motion capture modality is expensive, constrains motions to fit within the prescribed capture volume, is time consuming to set up and in processing marker position data, and is susceptible to dropped data due to marker occlusion. In sum, the current technology available in sport, clinical, and research contexts for quantifying three dimensional body segment orientation is expensive, may influence a subject's behavior, requires a long data reduction/processing time, constrains the activities being analyzed, and requires a skilled operator.

Some or all of these shortcomings may be addressable by advancing an alternative technology, namely miniaturized inertial measurement units (IMUs). Miniature IMUs incorporate MEMS accelerometers, angular rate gyros, and sometimes magnetometers which measure the translational acceleration, angular velocity, and local magnetic field of any body (including human body segments) to which they are attached. Relative to alternative modalities (e.g. MOCAP), this technology is inexpensive, does not require a skilled operator, is incredibly small (does not influence subject behavior), and can be deployed outside the research laboratory in naturalistic and clinical environments.

The accelerometer, rate gyro, and magnetometer incorporated in each IMU node enable independent estimates of the orientation of the node, and therefore the orientation of the object to which the node is attached. However, these orientation estimates can be incomplete or error prone. For example, the accelerometer data provides a noisy estimate of the IMU's orientation relative to gravity corrupted by the accelerations experienced by the device. Similarly, the magnetometer provides a noisy estimate of the IMU's orientation relative to magnetic north corrupted by local magnetic disturbances. Alternatively, integration of the gyro data provides a low-noise estimate of the change in the device's orientation, but subject to an unbounded time-varying drift error. Fusing the orientation estimates from each device, typically through a complementary or Kalman filtering framework, enables correction of gyro drift and an accurate identification of the orientation of the IMU. For example, two commercial systems (APDM Opal [9] and Xsens MVN [10]) use Kalman filtering to fuse accelerometer, rate gyro, and magnetometer data in providing a corrected estimate of IMU orientation. A recent study reveals the accuracy of the Xsens MVN for estimating rotations across the hip, knee, and ankle during level walking, stair ascent, and stair descent as compared to gold standard motion capture [11]. Unfortunately, these (and other) commercial IMU systems rely on proprietary algorithms requiring the use of prescribed hardware, which is range and sampling rate limited, and the use of magnetometer data which is highly sensitive to local magnetic field disturbances. To avoid magnetic field issues, a fusion of only accelerometer and rate gyro data can be used to correct for orientation drift. A recent study assessed the accuracy of several popular magnetometer-free drift correction techniques by comparing IMU and MOCAP estimates of pelvis, thigh, and shank orientation during maximal hip flexion, hip abduction, walking, squatting, and standing on one leg [8]. Similar to the aforementioned commercial systems, the algorithm yielding superior performance employs Kalman filtering which is complicated to implement and, due to large state vectors, requires significant computational load [12]. An attractive alternative is the complementary filter, which is less complex, yet provides similar levels of performance [12]. Several studies explore the use of complementary filters for fusing accelerometer and gyro data to correct orientation drift, see for example [12–15]. However, only [12] compares estimated results against gold standard optical motion capture and, unfortunately, only a subset of the orientation results are presented, effectively ignoring the remaining drift error.

Herein, we present a complementary filtering algorithm for fusing data from an accelerometer and angular rate gyro to estimate the orientation of an IMU. This technique improves upon existing, magnetometer based, corrections because it is unaffected by local magnetic field variations. We establish the validity of this algorithm by comparing IMU and MOCAP estimates of the orientation of a subject's torso or rifle during two tasks: 1) an up-down motion, commonly executed by soldiers, biathletes, and in sports like football or rugby where transitions from prone to standing (or the opposite) are often executed, and 2) a rifle aiming motion, commonly executed by soldiers, hunters, and biathletes. We also quantify remaining sources of error to highlight possible limitations of this approach. We open with a description of the subjects and tasks considered in our experiments.

METHODS

Human subjects

Sixteen subjects were recruited for participation from the local university population. Prior to testing, informed consent was obtained from each participant and approval was obtained from the University of Michigan Institutional Review Board.

Benchmarking Tasks

During testing, each subject completed four rounds of two benchmarking tasks. The first task, a simulated up-down maneuver, consisted of five maximal effort get-down-get-up cycles (from standing to lying prone back to standing). Each subject was instructed to pause momentarily in the standing and prone positions before transitioning. The second task consisted of rapidly aiming a mock rifle five times at two targets 15 feet from the subject and 180 degrees apart. Subjects were instructed to transition between targets as quickly as possible following an auditory cue. Each of these tasks was repeated four times per subject, during which the orientation of the

subject's torso or rifle was tracked using both an IMU and an optical motion capture system. This testing protocol yielded 64 trials for comparison.

Orientation of the Torso and Rifle

The orientation of a subject's torso and rifle during the described tasks is defined by the direction cosine matrix $C_{G/I}$ which quantifies the orientation of a ground-fixed reference frame, *G*, defined by the orthogonal triad of unit vectors ($\hat{E}_1, \hat{E}_2, \hat{E}_3$), relative to a body-fixed frame, *I* defined by the orthogonal triad ($\hat{e}_1, \hat{e}_2, \hat{e}_3$). The evolution of that direction cosine matrix in time is governed by

$$\frac{d}{dt} C_{G/I} = C_{G/I} \vec{\omega}^{\times} \tag{1}$$

where $\vec{\omega}^{\times}$ is the angular velocity of *I* relative to *G* represented as a skew symmetric matrix [16]. Provided that the initial orientation and the angular velocity (as a function of time) are known, one can solve Eq. (1) for $C_{G/I}$. Commonly, the angular velocity in Eq. (1) is directly measured by an IMU and used to compute its orientation as a function of time, see for example [1].

The IMU used in this study was a commercially available YEI 3-Space sensor (Yost Engineering, Portsmouth, Ohio). This device measures angular rates up to 2000 deg/s, with 16-bit resolution, and a 0.03 deg/sec/√Hz noise floor and accelerations up to 6 g, with 14-bit resolution, and a 650 μg/√Hz noise floor. Prior to use, the IMU was calibrated following the procedure detailed in [17]. This procedure, which consists of two rotations about each of the three orthogonal sense axes, determines 24 calibration parameters (including scale factors, cross-axis sensitivity scale factors, and biases) for the IMU components. Doing so ensures that the acceleration and angular rate measurements are accurately resolved along a common orthogonal triad, the body-fixed frame ($\hat{e}_1, \hat{e}_2, \hat{e}_3$). Bias values for the rate gyro are updated at the start of each trial to ensure that changes due to temperature, battery voltage, or other external factors are captured. Data were written to flash memory on the device and subsequently downloaded to a computer via USB upon completion of all trials for a given subject. For the aforementioned benchmarking tests, the IMU was secured to a motion capture marker frame (Fig. 1) before being attached to a subject's torso or rifle. Care was taken to align the sense axes of the IMU ($\hat{e}_1, \hat{e}_2, \hat{e}_3$) with the reference directions of the marker frame.

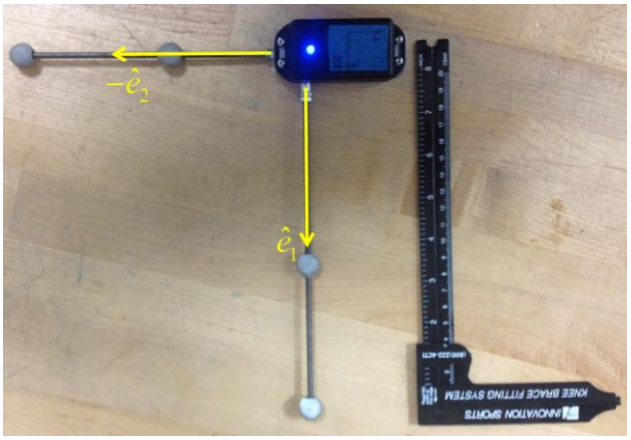

Figure 1: IMU and attached MOCAP marker frame used to provide comparison data for this benchmarking study. Two components of the body-fixed reference frame (*I*) are indicated by the orthogonal unit vectors $\hat{e}_1$ and $\hat{e}_2$.

In theory, the IMU provides direct measurement of the true angular velocity ($\vec{\omega}$) of the IMU and translational acceleration ($\vec{a}$) experienced at the accelerometer located therein. In practice, the measured angular velocity ($\vec{\omega}_m$) can be modeled as a linear combination of the true angular velocity, a bias ($\vec{\omega}_b$), and white noise ($\vec{\omega}_n$) per

$$\vec{\omega}_m = \vec{\omega} + \vec{\omega}_b + \vec{\omega}_n \tag{2}$$

Similarly, the measured acceleration ($\vec{a}_m$) can be modeled as a linear combination of the true translational acceleration of the device, the acceleration due to gravity ($\vec{g}$), and white noise ($\vec{a}_n$) per

$$\vec{a}_m = \vec{a} + \vec{g} + \vec{a}_n \tag{3}$$

The goal of sensor fusion is to use $\vec{a}_m$ to estimate $\vec{\omega}_b$ and $\vec{\omega}_n$ and remove them from the measured gyro signal yielding the true angular velocity which can then be used to identify the true orientation of the IMU, and in this context, the orientation of a subject's torso and rifle. Substitution of Eq. (2) into Eq. (1) yields the evolution equation governing the fused direction cosine matrix

$$\frac{d}{dt} C_{G/I} = C_{G/I} \left(\vec{\omega}_m - \vec{\omega}_b + K_P \vec{\theta}_e \right)^{\times} \tag{4}$$

and the evolution equation of the angular velocity bias

$$\frac{d}{dt} \vec{\omega}_b = -K_I \vec{\theta}_e \tag{5}$$

where $\vec{\theta}_e$ denotes an error identified by comparing the directions of gravity predicted by the accelerometer and the rate gyro, K_P is a proportional gain used in accounting for $\vec{\omega}_n$,

and K_I is an integral gain used in estimating $\vec{\omega}_b$. Equations (4) and (5) are adapted from [14] to provide an estimate of the true orientation, $C_{G/I}$ (via solution of Eq. (4)), following identification of the initial conditions for the direction cosine matrix and rate gyro bias.

These initial conditions are established during a time period at the start of a trial when the IMU attached to the torso or rifle is held stationary. Examination of Eq. (2) demonstrates that averaging $\vec{\omega}_m$ over this period yields the initial condition for $\vec{\omega}_b$. Similarly, averaging $\vec{a}_m$ over this period yields the direction of gravity relative to *I*, which we use to establish the initial orientation of $\hat{E}_3$. The projection of $\hat{e}_2$ onto the horizontal plane is used to establish the initial orientation of $\hat{E}_2$, while $\hat{E}_1 = \hat{E}_2 \times \hat{E}_3$. These three reference directions fully define the initial condition for $C_{G/I}$. Subsequently, the direction cosine matrix is determined from Steps 1-4 as follows.

Step 1: Estimate Gravity from the Accelerometer Measurement

From Eq. (3), the accelerometer provides a measurement of the direction of gravity ($\vec{g}$) corrupted by the acceleration of the device and white noise in the signal. Accordingly, at time t, the approximate gravity direction is defined as

$$\vec{g}_a(t) = \vec{a}_m(t) \big/ \left|\vec{a}_m(t)\right| \tag{6}$$

where $\left|\vec{a}_m(t)\right|$ is the vector magnitude of the accelerometer measurement.

Step 2: Propagate the Orientation of the Device

Simultaneously, the true angular velocity of the IMU can be estimated via

$$\tilde{\vec{\omega}}(t) = \vec{\omega}_m(t) - \tilde{\vec{\omega}}_b(t - dt) \tag{7}$$

where $\tilde{\vec{\omega}}(t)$ is an initial estimate of the true angular velocity, and the bias estimate from the previous time step ($t - dt$) is used to approximate the bias estimate at the current time step. This angular velocity estimate is then used to inform a solution to Eq. (1) using the numerical integration technique described in [1], which yields an estimate of the direction cosine matrix $\tilde{C}_{G/I}(t)$. The direction of gravity, as estimated by rate gyro data, is then defined per

$$\vec{g}_\omega(t) = \tilde{C}^T_{G/I}(t)\hat{E}_3 \tag{8}$$

Step 3: Calculate Misalignment of the Gravity Direction

An estimate of the effects of $\vec{\omega}_b$ and $\vec{\omega}_n$ on the gyro-predicted direction of gravity is then defined via the cross product

$$\vec{\theta}_e(t) = \vec{g}_a(t) \times \vec{g}_\omega(t) \tag{9}$$

where $\vec{\theta}_e(t)$ defines a rotation axis used to align the accelerometer and gyro predictions of gravity, whose magnitude is approximately the angle between $\vec{g}_a$ and $\vec{g}_\omega$.

Step 4: Estimate the True Angular Velocity

Simple numerical integration of (5) yields the following solution

$$\tilde{\vec{\omega}}_b(t) = \tilde{\vec{\omega}}_b(t - dt) - K_I \vec{\theta}_e(t)\, dt \tag{10}$$

where $\tilde{\vec{\omega}}_b$ is an estimate of the instantaneous gyro bias (updated from Step 2), and dt is the time between consecutive samples of data. Substitution of $\tilde{\vec{\omega}}_b(t)$ and $\vec{\theta}_e(t)$ into Eq. (4) enable a numerical solution (via the method in [1]) for the fused estimate of the direction cosine matrix at time t, $C_{G/I}(t)$. Steps 1-4 are repeated at each time step providing the orientation of the rifle and torso as functions of time during the benchmarking trials.

The primary assumption of this technique, made in Step 1, is that the accelerometer is measuring only the acceleration due to gravity (i.e. $\vec{a} = 0$). Unfortunately, at some points during the trial, the translational acceleration of the device is significant relative to gravity and, as a result, the direction of gravity estimated in Eq. (6) is flawed. This causes substantial error in Steps 2-4. To combat this, we adopt variable gains, where K_P and K_I are non-zero when the IMU is a rest and identically zero otherwise. The rest points are identified by considering instances during the trial when the magnitude of $\vec{\omega}_m$ and $\vec{a}_m$ are within the sensor noise floors of their stationary values. When the device is in motion, setting the gains to zero yields an estimate of bias equal to its value at the last rest point, but otherwise, the solution to Eq. (4) proceeds as described above. Steps 1-4 were implemented in MATLAB (MathWorks, Natick, MA, USA), and $C_{G/I}$ was estimated for each of the 64 trials.

Truth Orientation Data

Truth orientation data was obtained by tracking the 3D position of the reflective markers shown in Fig. 1 using an 8-camera VICON optical motion capture system (VICON Motion Systems, Oxford, UK). Positional measurements were recorded at a frequency of 100 Hz. These measurements were then used as input to a custom MATLAB program which constructs the direction cosine matrix $C_{G/I}$ at every sampling instant, enabling a direct comparison to the orientation derived from the IMU. Specifically, as evident from Fig. 1, the difference in three-dimensional marker positions yields estimates of $\hat{e}_1$ and $\hat{e}_2$,

which we refer to as $\tilde{\hat{e}}_1$ and $\tilde{\hat{e}}_2$, respectively. To ensure orthogonality in the MOCAP estimates of the body-fixed reference directions, we assume $\hat{e}_1 = \tilde{\hat{e}}_1$, and then construct a refined prediction by first establishing the direction of $\hat{e}_3$ according to

$$\hat{e}_3 = \hat{e}_1 \times \tilde{\hat{e}}_2 \Big/ \left| \hat{e}_1 \times \tilde{\hat{e}}_2 \right| \tag{11}$$

Finally, we construct $\hat{e}_2 = \hat{e}_3 \times \hat{e}_1$. These MOCAP estimates of the body-fixed reference directions are resolved in the MOCAP ground-fixed frame (*M*), which provides exactly the direction cosine matrix describing the orientation of the IMU relative to the MOCAP ground frame $C_{M/I}$. The MOCAP ground frame (*M*) is misaligned from the IMU ground frame (*G*) by a fixed rotation identified when the device is stationary at the start of each trial according to

$$C_{G/M} = C_{G/I}(0) C^T_{M/I}(0) \tag{12}$$

where $C_{G/M}$ is the fixed rotation from *M* to *G*, $C_{G/I}(0)$ is the initial orientation of *I* relative to *G*, and $C^T_{M/I}(0)$ is the initial orientation *M* relative to *I*. This fixed rotation allows us to identify the MOCAP estimate of $C_{G/I}(t)$ which is then used to calculate the task-specific torso and rifle angles used for comparison.

Torso and Rifle Angles

To assess the accuracy of the proposed algorithm for estimating the orientation of a subject's rifle and torso, we compare rifle elevation and azimuthal, and torso pitch angles as calculated from IMU and MOCAP data. As illustrated in Fig. 2, the rifle elevation angle is defined as the angle between the barrel of the rifle and the horizontal plane, while the azimuthal angle is defined as the angle formed between the projection of the rifle barrel on the horizontal plane and a reference line fixed in that plane. Similarly, torso pitch is defined as the angle formed between a subject's spine and vertical. We open the results section with comparisons of these angles calculated from IMU and MOCAP data.

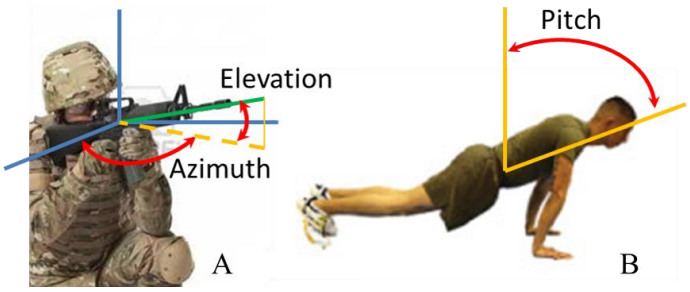

Figure 2: Definition of the rifle elevation and azimuthal (A) and torso pitch (B) angles used to assess accuracy of proposed orientation algorithm.

RESULTS

Figure 3A illustrates the torso pitch angle as calculated from IMU (red) and MOCAP (blue) data during a representative up-down trial, with example down and up motions highlighted. The agreement between the two motion sensing modalities is further evidenced by the correlation plot of Fig. 3B, where IMU pitch angle is plotted against its MOCAP counterpart. A red line with unit slope and zero intercept is added for reference.

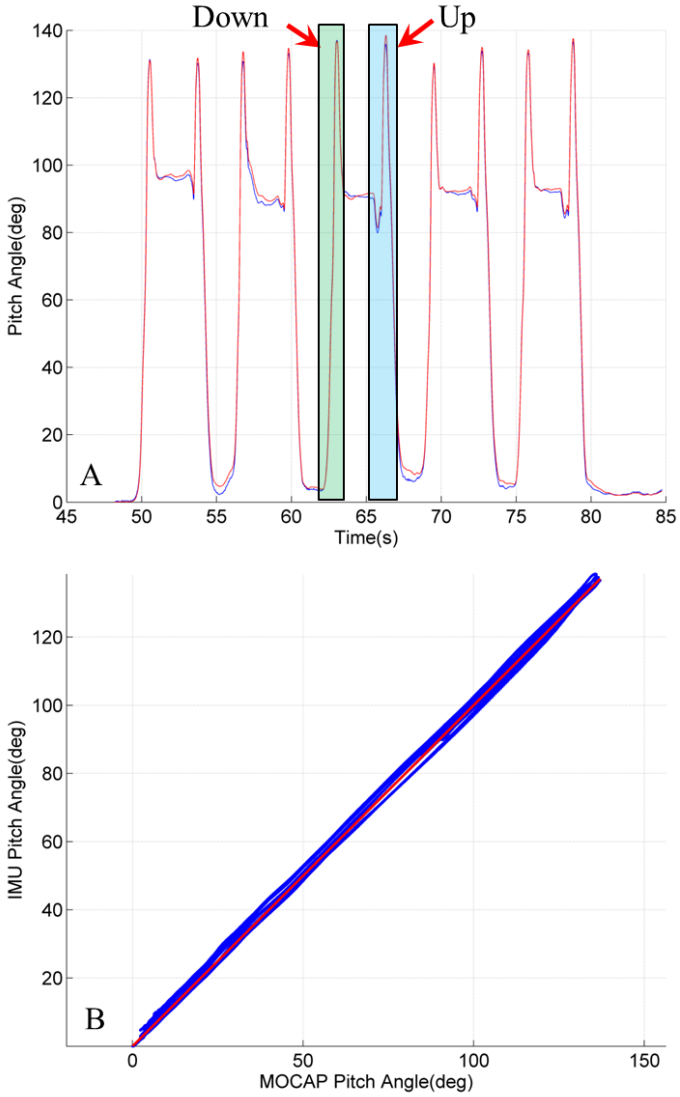

Figure 3: Torso pitch angle as a function of time (A) as estimated from IMU (blue) and MOCAP (red) data, example 'down' and 'up' motions are highlighted. Correlation plot (B) of IMU angle against MOCAP angle, where a red line with unit slope and zero intercept is added.

The IMU and MOCAP estimates of the torso pitch angle are nearly identical for this trial, as evidenced by the fact that the blue and red curves of Fig. 3A nearly superimpose exactly, and

the cloud of blue points in Fig. 3B nearly collapses to the (red) reference line. These results extend to the full data set (64 trials total: 4 trials/subject), where the average mean (SD) difference in the torso pitch angle is 0.55 (1.65) degrees. Table 1 summarizes the results for the 64 tests by reporting the mean (SD) of the mean and standard deviation of the difference in the torso pitch angle, as well as the mean (SD) of the slope, and R^2 of the best-fit line to the correlation plot data.

Similar results are observed for the rifle as illustrated in Fig. 4A, which reports the elevation (blue) and azimuthal (red) angles as calculated from IMU (dashed) and MOCAP (solid) data during a representative trial, with the turn and aim phases indicated. As the difference between the sets of curves is difficult to distinguish in Fig. 4A, it is specifically reported in Fig. 4B, along with the best-fit line for each. The beginning of each turn is further identified by the black dots in Fig. 4.

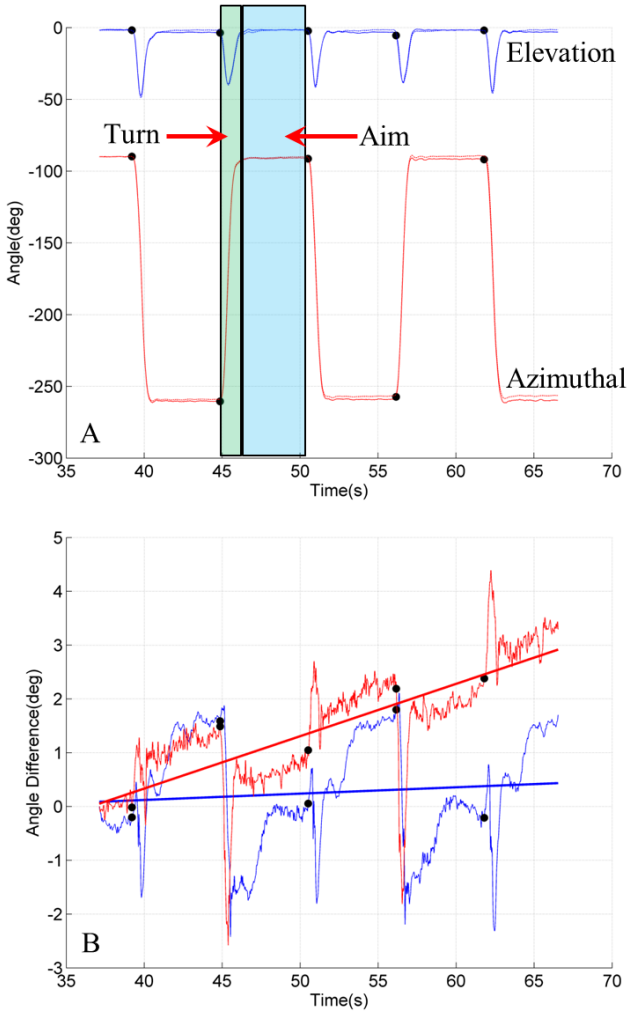

Figure 4: Rifle elevation (blue) and azimuthal (red) angle trajectories (A) as estimated from IMU (dashed) and MOCAP (solid) data. Angular difference between IMU and MOCAP estimates (B) of the elevation (blue) and azimuthal (red) angles with a linear fit to each added. The start of each turn is indicated by a black dot.

As with torso pitch, Fig. 4 demonstrates that the IMU orientation algorithm accurately estimates the rifle elevation angle. In contrast, as illustrated in Fig. 4B, the estimated azimuthal angle is still corrupted by drift error. Despite residual drift, the differences between IMU and MOCAP estimates for both the elevation and azimuthal angles remain quite small as is reflected in Table 1, which summarizes results for the full data set. In particular, Table 1 reports that the average mean (SD) difference in the rifle elevation and azimuthal angles are 0.44 (1.08) and 1.26 (1.54) degrees, respectively. This excellent agreement is also apparent in Fig. 5 which includes correlation plots for the elevation (Fig. 5A) and azimuthal (Fig. 5B) angles.

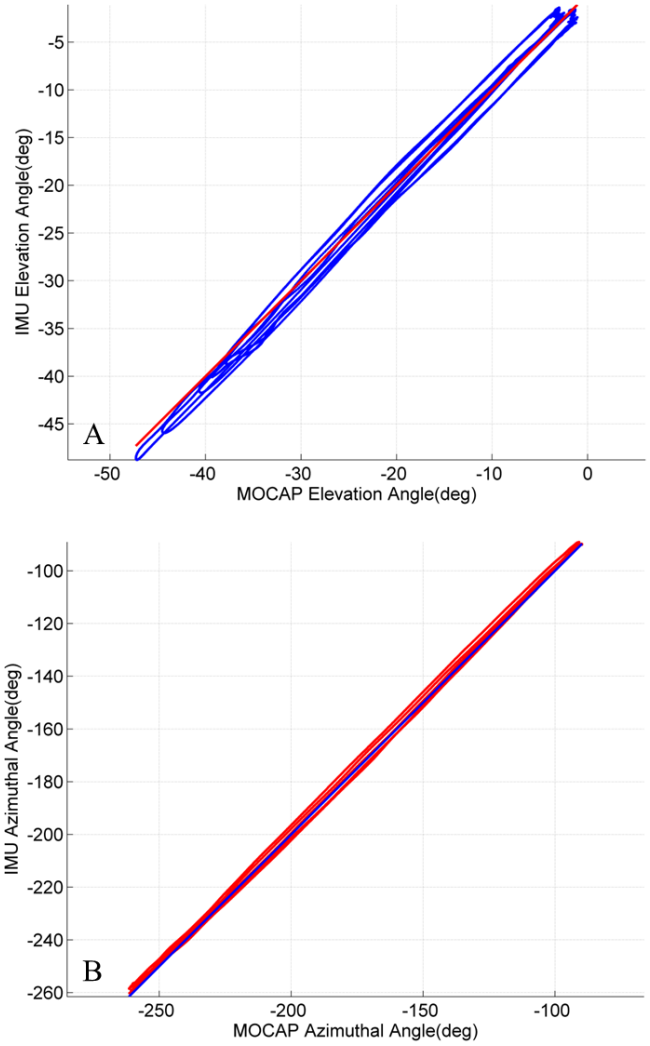

Figure 5: Correlation plots of IMU-estimated elevation (A) and azimuthal (B) angles plotted against their MOCAP counterparts, where red (A) and blue (B) lines with unit slope and zero intercept are added.

Again, despite residual drift error in the IMU azimuthal angle estimate, the data reported in Fig. 5 nearly collapse to their reference lines indicating excellent agreement. The mean (SD)

of the slope, and R^2 of the best-fit line to the correlation plot data for all trials are reported in Table 1.

Metric	Mean (deg)	SD (deg)	Slope	R^2
Torso Pitch	0.55 (0.52)	1.65 (0.57)	0.99 (0.01)	1.00 (0.00)
Rifle Elevation	0.44 (0.25)	1.08 (0.34)	0.95 (0.13)	0.92 (0.14)
Rifle Azimuth	1.26 (2.00)	1.54 (0.71)	0.99 (0.00)	1.00 (0.00)

Table 1: Agreement between IMU and MOCAP estimates of the torso pitch and rifle elevation and azimuthal angles summarized by the mean (SD) of the mean and SD of the difference and the slope and R^2 of the best-fit line to the correlation plot data.

Figure 6 illustrates the strong dependence of the rifle elevation angle slope and R^2 on the range of the elevation angle. Specifically, the slope (Fig. 6A) and R^2 (Fig. 6B) are plotted against the range of the elevation angle for each trial summarized in Table 1. For larger elevation angle ranges, the slope and R^2 approach 1.00.

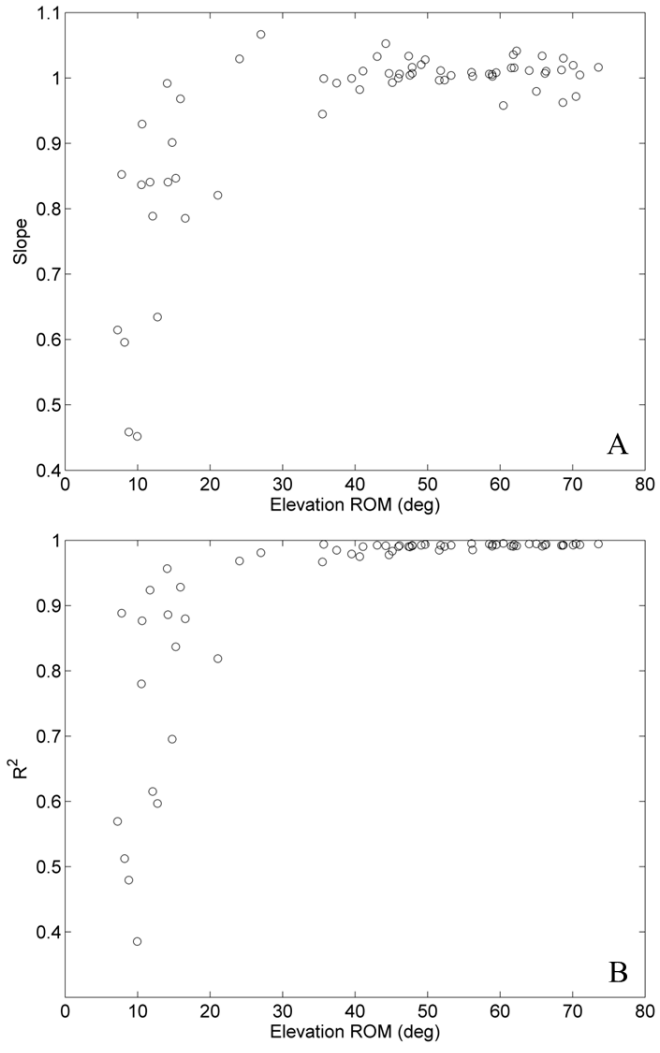

Figure 6: Rifle elevation angle slope (A) and R^2 (B) of the best-fit line to the correlation plot data versus range of motion for each trial.

We further quantify the difference between IMU and MOCAP estimates of the rifle elevation and azimuthal angles, as reported in Fig. 4B, by fitting a line to the angle difference as a function of time. Drift error has been shown to vary slowly with time [18,19], so the linear fit to the angle difference (IMU versus MOCAP) is an apt approximation of the residual drift error. The mean (SD) of the intercept, slope magnitude, and R^2 of the fits for each of the trials considered are reported in Table 2.

Metric	Intercept (deg)	|Slope| (deg/s)	R^2
Torso Pitch	0.19 (0.78)	0.01 (0.01)	0.02 (0.02)
Rifle Elevation	-0.14 (0.44)	0.01 (0.01)	0.01 (0.01)
Rifle Azimuth	-3.22 (5.66)	0.09 (0.13)	0.50 (0.32)

Table 2: Summary of linear regressions used to approximate the drift error in each trial based on angle difference data including the mean (SD) of the intercept, magnitude of the slope, and R^2.

DISCUSSION

A complementary filter based IMU orientation drift correction algorithm is introduced herein and its accuracy is established by considering the angular displacement of the torso and rifle during tasks commonly employed by warfighters and athletes. We discuss the results for the torso pitch, and rifle elevation and azimuthal angles that establish the validity of our correction algorithm and compare them to existing work. Furthermore, we discuss likely sources of the remaining error in these angle estimates and comment on the limitations of this approach.

Validity of Orientation Correction

The accuracy of the correction algorithm is established in Table 1. Across all trials (N=64), the average mean (SD) difference between the IMU and MOCAP estimates of the torso pitch and rifle elevation angles are 0.55 (1.65) and 0.44 (1.08) degrees, respectively. The excellent agreement in these angles is further confirmed by the average slope (R^2) values across all trials. For the pitch angle, the average slope of the best-fit line is 0.99, and on average, nearly 100% of the variance in the IMU estimated pitch angle is explained by the MOCAP pitch angle. In contrast, the elevation angle has an average slope for the best-fit line of 0.95, and 92% of the variation in the IMU elevation angle is explained by the MOCAP angle. This discrepancy in regression parameters is surprising as the pitch and elevation angles are both defined relative to gravity (pitch angle relative to vertical versus elevation angle relative to horizontal), and both employ the same drift correction algorithm. Moreover, the mean differences in the pitch and elevation angles are not significantly different ($t = -1.59$, $p = 0.12$). Figure 6 reveals the root cause of this discrepancy. Specifically, when the range of the elevation angle is small (< 25 degrees) the linear regression is poorly conditioned, resulting in slope and R^2 values further from 1. In contrast, the range of the torso pitch angle is guaranteed to be at least 90 degrees, a constraint imposed by the up-down motion

itself, which leads to a well-conditioned linear regression. Neglecting the 18 trials with elevation angle ranges less than 25 degrees, the mean (SD) slope and R^2 values improve to 1.01 (0.02) and 0.99 (0.01), respectively, which agree well with the pitch results.

For the rifle azimuthal angle, the average mean (SD) difference between the IMU and MOCAP estimates is 1.26 (1.54) degrees which is significantly greater than the mean differences observed for the elevation and pitch angles. Nevertheless, an average difference on the order of one degree represents an exceptional estimate for many purposes. The agreement is further confirmed by the average slope and R^2 value across all trials. The average slope of the best-fit line is 0.99, and on average, nearly 100% of the variation in the IMU estimate is explained by the MOCAP estimate which is likely due to the fact that the range of the azimuthal angle (at least 180 degrees) is significantly larger than any error in the estimate over the trial times (approximately 30 seconds) considered herein.

The results above compare favorably with existing magnetometer-free sensor fusion techniques for IMU orientation drift correction. For example, the best drift correction technique employed in [8] achieves mean and standard deviation errors of 2-3 degrees in the most successful task. A second orientation correction algorithm [20] estimates the IMU tilt angle (equivalent to the pitch and elevation angles) to within a mean (SD) RMS error of 1.9 (0.4) degrees for rotation ranges similar to those in this study. The mean (SD) RMS error for the pitch and elevation angles above are slightly better; namely 1.8 (0.6) and 1.2 (0.3) degrees, respectively. However, they are also slightly below the mean RMS errors of approximately 0.6 degrees reported in [12] for the significantly slower speed motions considered therein.

Despite the overall good agreement, the mean difference in the azimuthal angle estimate is significantly larger than that for the pitch and elevation angles. For instance, a paired sample t-test reveals a statistically significant ($t = -3.30$, $p = 0.002$) difference between the mean elevation and azimuthal angle results. This difference is attributed to residual drift error in the azimuthal angle as described next.

Remaining Error

Evidence of the remaining drift error in the azimuthal angle is illustrated in Fig. 4B, where the difference between the IMU and MOCAP estimates of this angle increases nearly linearly with time. This pattern is characteristic of drift error [1], in fact, orientation drift has previously been modeled as a linear function in time [20]. To identify the source of this drift error, we return to the gyro correction defined in Eq. (9). Note that this equation constrains corrections to the horizontal components of the angular velocity vector. The correction is applied relative to the body-fixed frame (*I*), but if the device is held at rest with one of its axes in the vertical direction, then the error along that axis remains unobservable. Unfortunately, the mounting of the IMU on the mock rifle nearly guaranteed that the $\hat{e}_3$ axis was approximately aligned with gravity while the rifle was held at rest, preventing estimation of an accurate bias correction along that axis. The $\hat{e}_3$ axis was also approximately aligned with gravity for the majority of the rifle aiming trial, and since the azimuthal angle corresponds to rotation about the vertical axis, residual drift remains in the azimuthal angle estimate.

For each trial, the resulting drift error is approximated by a linear function of time with the intercept, and slope (magnitude) listed in Table 2. From the arguments above, we expect greater drift in the azimuthal angle than in the elevation angle, and the reported results confirm these expectations. On average, the slope, or drift rate, in the elevation angle is 0.01 degrees/s, while the drift rate in the azimuthal angle is nearly an order of magnitude larger, namely 0.09 degrees/s. The difference in drift rate is statistically significant ($t = -4.77$, $p < 0.0001$). To provide context for the drift rates, consider the approximate drift error expected over the time duration of the rifle aiming task which lasted for 29.7 +/- 0.5 seconds. An approximate average drift error (drift rate times time duration) of 0.30 degrees is therefore expected for the elevation angle while 2.67 degrees is expected for the azimuthal angle.

Table 2 also reports the percentage of the variance in the angle difference explained (R^2) by the linear drift error approximation. On average, the drift error approximation explains 50% of the variance in the azimuthal angle difference and only 1% in the elevation angle difference. This discrepancy in explained variance is statistically significant ($t = -12.25$, $p < 0.0001$). The fact that so little of the variance in the elevation angle difference is explained by the drift error approximation suggests that the (very small) residual errors in the elevation angle derive from measurement noise and not drift. Thus, the drift correction works extremely well for the elevation angle and to a lesser degree for the azimuthal angle due to the limitations in error observability described above.

It is important to point out that the drift error approximation only accounts for 50% of the variation in the azimuthal angle difference, and only 1% of the difference in the elevation angle. To identify the remaining potential sources of error, we again consider Fig. 4, where the beginning of each turn phase is indicated by a black dot. Notice that immediately following the initiation of each turn, there is a large spike in the angle difference reported in Fig. 4B. During the turn, the IMU and the attached marker frame are subject to highly dynamic motion, which can induce deflections of the marker frame (Fig. 1) as well as increased errors in the MOCAP positional measurements. These errors in the MOCAP estimate of $C_{G/I}$ likely contribute significantly to the remaining difference in the angle estimates. Additionally, a small misalignment between the MOCAP frame reference directions and the true sense axes of the IMU could be responsible for some of the observed difference. These error sources are likely responsible for the

discrepancy between the results presented herein and those presented in [12] where the motions considered were far less dynamic.

Limitations and Future Work

As noted above, the algorithm corrects for drift in the IMU estimates of torso pitch and rifle elevation angles, and to a lesser degree for the rifle azimuthal angle. Future improvements may result from a different form of Eq. (9) that enables bias estimation in all three components of the angular velocity regardless of IMU orientation or by considering supplementary measurement data (i.e. magnetometer data, etc.). Additionally, note that movements considered herein, while representative of the target applications, are also not exhaustive of all possible movements. In particular, the movements included significant periods during which the subject was at rest allowing the orientation algorithm to successfully identify and remove drift error. However, should movements have far fewer or shorter rest periods, or longer intervals of time between rest periods, poorer estimates would likely result.

CONCLUSION

We present a simple complementary filtering algorithm for fusing data from an accelerometer and angular rate gyro to estimate the orientation of an IMU. The technique improves upon existing, magnetometer-based corrections because it is unaffected by local magnetic field variations. We establish the validity of this algorithm by comparing IMU and MOCAP estimates of the orientation for two representative tasks; namely up/down motions and rifle aiming. Results reveal that this filtering yields torso pitch angles that remain within 0.55 degrees of MOCAP estimates and rifle elevation and azimuthal angles that remain within 0.44 and 1.26 degrees on average, respectively, for the 64 trials analyzed. We further examine the residual drift error in the angle estimates and demonstrate that, for the pitch and elevation angles, drift is largely removed. These promising results point to the future use of this technology for quantifying human motion in natural settings, for example on the field of play/training. Their use may be extended to other applications including remote health monitoring where noninvasive, inexpensive, and accurate methods for reliable orientation estimation are desired.

ACKNOWLEDGMENTS

Funding for this study provided by the US Army Natick Soldier Research, Development and Engineering Center - Contract # W911QY-13-C-0011.

REFERENCES

[1] McGinnis, R. S., and Perkins, N. C., 2012, "A highly miniaturized, wireless inertial measurement unit for characterizing the dynamics of pitched baseballs and softballs," Sensors, **12**(9), pp. 11933–11945.

[2] King, K., Hough, J., McGinnis, R., and Perkins, N., 2012, "A new technology for resolving the dynamics of a swinging bat," Sports Eng., **15**(1), pp. 41–52.

[3] King, K., Perkins, N. C., Churchill, H., McGinnis, R., Doss, R., and Hickland, R., 2010, "Bowling ball dynamics revealed by miniature wireless MEMS inertial measurement unit," Sports Eng., **13**(2), pp. 95–104.

[4] McGinnis, R. S., and Perkins, N. C., "Inertial sensor based method for identifying spherical joint center of rotation," J. Biomech.

[5] McGinnis, R., Cain, S., Tau, S., Whiteside, D., Goulet, G., Gardner, E., Perkins, N., and Bedi, A., "Validation of a Novel IMU-based Three-dimensional Hip Angle Measurement in Diagnostic Tests for Femoroacetabular Impingement," J. Biomech., **Submitted**.

[6] Gross, M. M., Crane, E. A., and Fredrickson, B. L., 2012, "Effort-Shape and kinematic assessment of bodily expression of emotion during gait," Hum. Mov. Sci., **31**(1), pp. 202–221.

[7] Simon, S. R., 2004, "Quantification of human motion: gait analysis—benefits and limitations to its application to clinical problems," J. Biomech., **37**(12), pp. 1869–1880.

[8] Öhberg, F., Lundström, R., and Grip, H., 2013, "Comparative analysis of different adaptive filters for tracking lower segments of a human body using inertial motion sensors," Meas. Sci. Technol., **24**(8), p. 085703.

[9] "APDM Opal" [Online]. Available: http://apdm.com/products/movement-monitors/opal/.

[10] "Xsens MVN - Products," Xsens 3D Motion Track.

[11] Zhang, J.-T., Novak, A. C., Brouwer, B., and Li, Q., 2013, "Concurrent validation of Xsens MVN measurement of lower limb joint angular kinematics," Physiol. Meas., **34**(8), p. N63.

[12] Madgwick, S. O. H., Harrison, A. J. L., and Vaidyanathan, A., 2011, "Estimation of IMU and MARG orientation using a gradient descent algorithm," IEEE Int. Conf. Rehabil. Robot. Proc., **2011**, p. 5975346.

[13] Mahony, R., Hamel, T., and Pflimlin, J.-M., 2005, "Complementary filter design on the special orthogonal group SO(3)," 44th IEEE Conference on Decision and Control, 2005 and 2005 European Control Conference. CDC-ECC '05, pp. 1477–1484.

[14] Mahony, R., Hamel, T., and Pflimlin, J.-M., 2008, "Nonlinear Complementary Filters on the Special Orthogonal Group," IEEE Trans. Autom. Control, **53**(5), pp. 1203–1218.

[15] Euston, M., Coote, P., Mahony, R., Kim, J., and Hamel, T., 2008, "A complementary filter for attitude estimation of a fixed-wing UAV," IEEE/RSJ International Conference on Intelligent Robots and Systems, 2008. IROS 2008, pp. 340–345.

[16] Greenwood, D. T., 1965, Principles of dynamics, Prentice-Hall, Englewood Cliffs, N.J.

[17] King, K. W., 2008, "The design and application of wireless MEMS inertial measurement units for the measurement and analysis of golf swings," PhD, University of Michigan.
[18] Savage, P., 2000, Strapdown analytics, Strapdown Associates, Maple Plain, MN.
[19] Titterton, D. H., and Weston, J. L., 2004, Strapdown inertial navigation technology, Institution of Electrical Engineers, Stevenage, UK.
[20] Favre, J., Jolles, B. M., Siegrist, O., and Aminian, K., 2006, "Quaternion-based fusion of gyroscopes and accelerometers to improve 3D angle measurement," Electron. Lett., **42**(11), pp. 612– 614.